

Universal Features of Spin Transport and Breaking of Unitary Symmetries

Ph. Jacquod¹ and İ. Adagideli²

¹*Physics Department, University of Arizona, 1118 E. 4th Street, Tucson, AZ 85721, USA*

²*Faculty of Engineering and Natural Sciences, Sabanci University, Orhanli-Tuzla, Istanbul, Turkey*

(Dated: October 8, 2018)

When time-reversal symmetry is broken, quantum coherent systems with and without spin rotational symmetry exhibit the same universal behavior in their electric transport properties. We show that spin transport discriminates between these two cases. In systems with large charge conductance, spin transport is essentially insensitive to the breaking of time-reversal symmetry. However, in the opposite limit of a single exit channel, spin currents vanish identically in the presence of time-reversal symmetry, but are turned on by breaking it with an orbital magnetic field.

PACS numbers: 72.25.Dc, 73.23.-b, 75.76.+j

Introduction. Fifty years ago, Dyson showed that ensembles of unitary matrices that are invariant under general symmetry groups reduce to the direct product of three irreducible ensembles [1]. These three circular ensembles are labelled by an index $\beta = 1, 2, 4$ and are respectively invariant under the transformations

$$S \rightarrow U^T S U, \text{ orthogonal ensemble, } \beta = 1, \quad (1a)$$

$$S \rightarrow U S V, \text{ unitary ensemble, } \beta = 2, \quad (1b)$$

$$S \rightarrow W^R S W, \text{ symplectic ensemble, } \beta = 4, \quad (1c)$$

where S is an element of the ensemble, U and V are arbitrary unitary matrices, W is a quaternion [2] unitary matrix, U^T is the transpose of U and $W^R = \sigma^{(y)} W^T \sigma^{(y)}$ is the dual of W [3]. Here and below, $\sigma^{(\mu)}$, $\mu = x, y, z$ is a Pauli matrix. This classification carries over to electronic quantum transport [4], where the three classes are defined by time-reversal symmetry (TRS), an antiunitary symmetry. Systems without TRS have a scattering matrix in the $\beta = 2$ ensemble, while systems with TRS are differentiated by whether the TRS operator squares to $+1$ ($\beta = 1$) or -1 ($\beta = 4$). When TRS is preserved, breaking spin rotational symmetry (SRS) induces a crossover $\beta = 1 \rightarrow 4$, however when TRS is broken, breaking SRS only doubles the size of the scattering matrix as a Kramers degeneracy gets removed. This does not generate a new ensemble [1, 4, 5].

Quantum corrections to electric transport depend on the symmetry index β , but are independent of the size N of the scattering matrix (giving the total number of transport channels from and to the scatterer) for large N [4]. According to the above classification, universality in charge transport is therefore mostly determined by the antiunitary TRS. Recent investigations of spin transport showed that the magnetoelectric spin conductance

$$\mathcal{T}_{ij}^{(\mu)} = \text{Tr}[S_{ij}^\dagger \sigma^{(\mu)} S_{ij}], \quad (2)$$

constructed from the transmission block S_{ij} of the scattering matrix connecting terminals i and j , also exhibits a character of universality [6–10] in that $\text{var } \mathcal{T}_{ij}^{(\mu)} = 4N_i(N_i - 1)N_j/N(2N - 1)(2N - 3)$ for $\beta = 4$. Here, $N_{i,j}$

gives the number of transport channels between the system and terminals i, j , and $N = \sum_i N_i$. The spin conductance fluctuates about zero average, $\langle \mathcal{T}_{ij}^{(\mu)} \rangle = 0$ and the resulting, typically nonzero spin current is generated by the presence of a SRS breaking field. In the $\beta = 4$ ensemble one usually takes the latter field as spin-orbit interaction (SOI). In the absence of SOI, one has $\mathcal{T}_{ij}^{(\mu)} \equiv 0$. This is the case for $\beta = 1$ and, if Dyson's three-fold way applies to spin transport, for $\beta = 2$. In this manuscript we demonstrate that spin transport discriminates between systems with and without SRS even when TRS is broken. Accordingly, a novel kind of universality emerges in systems with broken SRS and TRS, with charge transport properties given by those of the $\beta = 2$ ensemble, but with specific spin transport properties. The latter are similar to those of the $\beta = 4$ ensemble at large N , a finding already reported in Ref. [11] for specific four-terminal setups, but deviate from it at small N . Our finding does not invalidate Dyson's classification—the latter gives a complete classification of unitary scattering matrices and unless one introduces chiral or particle-hole symmetries [12, 13], there is no new ensemble to be found. Instead our point is that spin-dependent observables define two sub-ensembles of the $\beta = 2$ ensemble, depending on whether they commute or not with the scattering matrix. In other words, we find that while universality in charge transport is affected only by the antiunitary TRS universality in spin transport depends on both antiunitary (TRS) and unitary (SRS) symmetries.

The model. We consider a mesoscopic conductor connected to any number of external electron reservoirs. There is no ferromagnetic exchange anywhere in the system, nor is there spin accumulation in the reservoirs, thus injected currents are not polarized. We neglect spin relaxation in the terminals. The magnetoelectrically generated spin current due to the presence of SOI inside the cavity is determined by the spin-dependent transmission coefficients of Eq. (2). For instance, in the simple case of a two-terminal setup, the generated spin current in the right lead along the polarization axis $\mu = x, y, z$ is given

by

$$I_{\text{R}}^{(\mu)} = (e^2 V/h) \mathcal{J}_{\text{RL}}^{(\mu)}, \quad (3)$$

with the voltage bias V applied across the sample.

Semiclassical calculation. We first calculate the average and mesoscopic fluctuations of the spin transmission coefficients using the semiclassical theory of transport [14, 15], extended to take spin transport into account [16, 17]. We write (See Supplemental Material [18])

$$\mathcal{J}_{ij}^{(\mu)} = \int_i dy \int_j dy_0 \sum_{\gamma, \gamma'} A_\gamma A_{\gamma'}^* e^{i(S_\gamma - S_{\gamma'})} \text{Tr}[U_\gamma \sigma^{(\mu)} U_{\gamma'}^\dagger]. \quad (4)$$

The sums run over all trajectories starting at y_0 on a cross-section of the injection lead j and ending at y on the exit lead i . Trajectories have a stability given by A_γ , which includes a prefactor $(2\pi i \hbar)^{-1/2}$ as well as a Maslov index [19], and S_γ gives the classical action accumulated on γ , in units of \hbar . SOI is incorporated in the matrices U_γ . The average spin conductance has been calculated semiclassically in Ref. [17]. In the absence of SOI, spins do not rotate, $U_\gamma = \sigma^{(0)}$ is the identity matrix, and one trivially obtains $\mathcal{J}_{ij}^{(\mu)} \equiv 0$. The leading-order approximation is to consider $U_\gamma \in \text{SU}(2)$, where SOI rotate the spin of the electron along unperturbed classical trajectories [16, 20]. In this manuscript, we will use this approximation because, even though it neglects the geometric correlations reported in Ref. [17], it is appropriate for our search of universality. At that level, the average spin conductance vanishes, $\langle \mathcal{J}_{ij}^{(\mu)} \rangle_{\text{semicl}} = 0$ [17], which agrees with the random matrix theory (RMT) result of Ref. [6].

Having established that the average spin conductance vanishes regardless of the presence or absence of TRS and SRS, we next calculate spin conductance fluctuations. The leading-order diagrams contributing to $\text{var}[\mathcal{J}_{\text{RL}}^{\mu 0}]_{\text{semicl}}$ are shown in Fig. 1. They are the same as those contributing to the (charge) transmission fluctuations [substituting $\sigma^{(\mu)} \rightarrow \sigma^{(0)}$ in Eq. (2)]. In this case, Ref. [15] found that the sum of contributions $c)$, $d)$ and $e)$ cancel out, furthermore, contribution $b)$ vanishes upon breaking of TRS. This can be achieved via a magnetic flux piercing the diagram's loop. From Fig. 1, we see that contribution $b)$ is the only one that is flux-sensitive, because the blue (dark) and the red (light) trajectories accumulate the same flux-phase. From a semiclassical point of view, this is the origin of the halving of the universal conductance fluctuations upon TRS breaking [4]. Extending this calculation to $\text{var}[\mathcal{J}_{ij}^\mu]_{\text{semicl}}$, we obtain that contributions $a)$, $b)$ and $c)$ are multiplied by a spin-dependent term $\text{Tr}[U_{\gamma_5}^\dagger U_{\gamma_3}^\dagger \sigma^{(\mu)} U_{\gamma_3} U_{\gamma_2}] \times \text{Tr}[U_{\gamma_2}^\dagger U_{\gamma_6}^\dagger \sigma^{(\mu)} U_{\gamma_6} U_{\gamma_5}]$, while contributions $d)$ and $e)$ are multiplied by $|\text{Tr}[U_{\gamma_5}^\dagger \sigma^{(\mu)} U_{\gamma_2}]|^2$ (See Supplemental Information for the labelling of trajectory segments [18]). All these terms vanish in the absence of SOI. In the presence

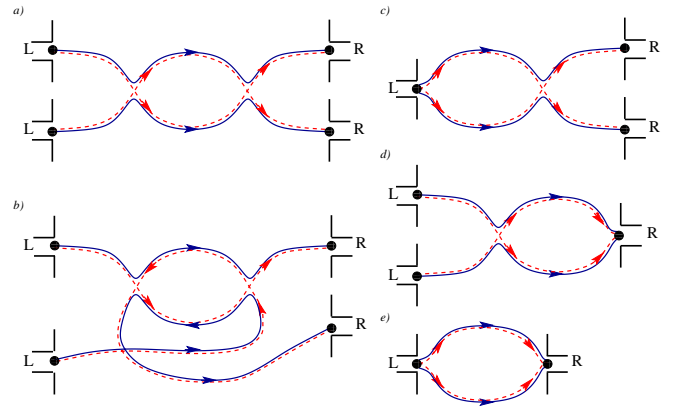


Figure 1: (Color online) Semiclassical diagrams determining the conductance and spin conductance fluctuations to leading order in the number $N \gg 1$ of transport channels. Blue (dark) and red (light) trajectories travel in opposite direction in diagram $b)$, which consequently vanishes in the presence of a large magnetic flux piercing the loop. All other diagrams are insensitive to the breaking of time-reversal symmetry.

of SOI, we evaluate them by averaging over a uniform distribution of all U_γ 's over the $\text{SU}(2)$ group, corresponding to totally broken SRS. Following the standard procedure of performing orbital averages and spin averages separately, we obtain that, when SRS is totally broken, contributions $a)$, $b)$ and $c)$ acquire a prefactor $\langle \dots \rangle_{\text{SU}(2)}$ indicates an homogeneous average over the $\text{SU}(2)$ group

$$\langle \text{Tr}[U_{\gamma_5}^\dagger U_{\gamma_3}^\dagger \sigma^{(\mu)} U_{\gamma_3} U_{\gamma_2}] \text{Tr}[U_{\gamma_2}^\dagger U_{\gamma_6}^\dagger \sigma^{(\mu)} U_{\gamma_6} U_{\gamma_5}] \rangle_{\text{SU}(2)} = 0, \quad (5)$$

and thus vanish identically, while contributions $d)$ and $e)$ are multiplied by

$$\langle |\text{Tr}[U_{\gamma_5}^\dagger \sigma^{(\mu)} U_{\gamma_2}]|^2 \rangle_{\text{SU}(2)} = 1. \quad (6)$$

We conclude that the semiclassical contributions to the spin conductance fluctuations are those with a correlated encounter at the exit terminal, which in particular has the consequence that they are not sensitive to the breaking of TRS.

We obtain the variance of the spin conductance coefficients as the sum of contributions $d)$ and $e)$, i.e.

$$\text{var}[\mathcal{J}_{ij}^{(\mu)}]_{\text{semicl}} = (N_i N_j N - N_i N_j^2) / N^3. \quad (7)$$

The key point is that this result holds both in the absence and in the presence of TRS, because both relevant contributions $d)$ and $e)$ are sensitive neither to magnetic fluxes piercing their loops, nor to orbital magnetic field effects that do not alter the ergodicity of the classical trajectories. Thus, Eq. (7) gives the leading-order semiclassical expression for the conductance variance, for systems without SRS (with SOI) in both cases of conserved or broken TRS, as well as in the intermediate regime of partially broken TRS. Therefore, to leading order in the number $N \gg 1$ of transport channels, spin conductance

fluctuations are insensitive to the breaking of TRS. In the next section, this result is confirmed using RMT.

Random matrix theory calculation. We next use the method of Ref. [21] to calculate the RMT average and fluctuations of the spin conductance. We write [6]

$$\mathcal{T}_{ij}^{(\mu)} = \text{Tr} [Q_i^{(\mu)} S Q_j^{(0)} S^\dagger], \quad (8a)$$

$$[Q_i^{(\mu)}]_{m\eta, n\nu} = \begin{cases} \delta_{mn} \sigma_{\eta\nu}^{(\mu)}, & m \in i \\ 0, & \text{otherwise,} \end{cases} \quad (8b)$$

$$[Q_j^{(\mu)}]_{m\eta, n\nu} = \begin{cases} \delta_{mn} \sigma_{\eta\nu}^{(\mu)}, & m \in j, \\ 0, & \text{otherwise,} \end{cases} \quad (8c)$$

where m and n are channel indices, η and ν are spin indices and $\sigma^{(0)}$ is the 2×2 identity matrix. The trace in Eq. (8a) is taken over both sets of indices. We find that the average of the spin transmission vanishes in all cases,

$$\langle \mathcal{T}_{ij}^{(\mu)} \rangle_{\text{RMT}} = 0. \quad (9)$$

For the $\beta = 4$ ensemble, this result was first obtained in Ref. [6]. We further obtain

$$\text{var}[\mathcal{T}_{ij}^{(\mu)}]_{\beta=2; \text{SRS}} = 0, \quad (10a)$$

$$\text{var}[\mathcal{T}_{ij}^{(\mu)}]_{\beta=2; \text{SRS}} = 4 \frac{N_i N_j N - N_i N_j^2}{N(4N^2 - 1)}, \quad (10b)$$

$$\text{var}[\mathcal{T}_{ij}^{(\mu)}]_{\beta=4} = 4 \frac{N_i N_j (N - 1) - N_i N_j^2}{N(2N - 1)(2N - 3)}. \quad (10c)$$

Eq. (10c) first appeared in Ref. [6], and expressions similar to Eq. (10b) appeared in Refs. [10, 11] for two-terminal geometries. We see that Eqs. (7), (10b) and (10c) all agree in the limit $N_{i,j} \gg 1$, however, while the semiclassical expression Eq. (7) is valid only in that limit, Eqs. (10) are exact for any number of channels. Most interestingly, for a two-terminal setup with $N_i = 1$, Eq. (10c) gives $\text{var}[\mathcal{T}_{ij}^{(\mu)}]_{\beta=4} = 0$. Together with Eq. (9) this gives an identically vanishing spin conductance, in agreement with Ref. [22]. This restriction no longer applies once TRS is broken, as reflected in Eq. (10b) – breaking TRS can turn spin currents in two-terminal geometries, when the exit terminal carries a single transport channel.

Numerical simulations. We numerically confirm our findings using the quantum mechanical spin kicked rotator model [23]. It is represented by a $2M \times 2M$ Floquet matrix [23–25] (See Supplemental Material [18])

$$\mathcal{F}_{ll'} = (\Pi U X U^\dagger \Pi)_{ll'}, \quad l, l' = 0, 1, \dots, M - 1, \quad (11a)$$

$$\Pi_{ll'} = \delta_{ll'} e^{-i\pi(l+l_0)^2/M} \sigma_0, \quad (11b)$$

$$U_{ll'} = M^{-1/2} e^{-i2\pi ll'/M} \sigma_0, \quad (11c)$$

$$X_{ll'} = \delta_{ll'} e^{-i(M/4\pi)V(2\pi l/M)}. \quad (11d)$$

The matrix Π represents free ballistic motion, periodically interrupted by spin-independent and spin-

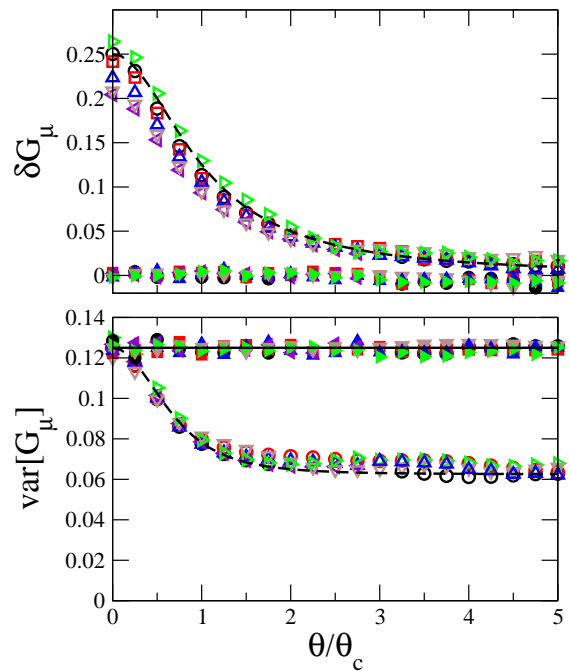


Figure 2: (Color online) Weak localization corrections to (top), and variance of (bottom) the charge (empty symbols) and spin (full symbols) conductance for the two-terminal quantum kicked rotator of Eqs. (11). Parameters are $\tau_D = 10, 20$, $K = 40, 60, 80, 90$, $K_{\text{so}} = 120 K_{\text{soc}}$ and $M = 128, 256, 512$. The dashed lines indicate the RMT predicted crossover from $\beta = 4$ to $\beta = 2$ [23]. Our semiclassical prediction of Eq. (7) is illustrated by the straight black line in the bottom panel. For all data, $N > 10$.

dependent kicks given by the matrix X , and corresponding to scattering at the boundaries of the quantum dot, as well as SOI. We choose

$$V(p) = K \cos(p + \theta) \sigma_0 + K_{\text{so}} (\sigma_x \sin 2p + \sigma_z \sin p). \quad (12)$$

The corresponding classical map is chaotic for kicking strength $K \gtrsim 7.5$, accordingly in our search for universal behavior, we restrict ourselves to that regime. The SO coupling strength K_{so} is related to the SO rotation time τ_{so} (in units of the stroboscopic period) through $\tau_{\text{so}} = 32\pi^2/K_{\text{so}}^2 M^2$ [23]. From (11), we construct the quasienergy-dependent scattering matrix as

$$S(\varepsilon) = P[e^{-i\varepsilon} - \mathcal{F}(1 - P^T P)]^{-1} \mathcal{F} P^T, \quad (13)$$

with P a $2N \times 2M$ projection matrix

$$P_{k\alpha, k'\beta} = \begin{cases} \delta_{\alpha\beta} & \text{if } k' = l^{(k)}, \\ 0 & \text{otherwise.} \end{cases} \quad (14)$$

The $l^{(k)}$ ($k = 1, 2, \dots, 2N$, labels the modes) give the position in phase space of the attached leads. The mean dwell time τ_D is given by $\tau_D = M/N$. The parameter K_{so} breaks SRS over a scale $K_{\text{soc}} = 4\pi\sqrt{2}/M\tau_D^{1/2}$ corresponding to $\tau_{\text{so}} = \tau_D$, and θ breaks time-reversal symmetry over a scale $\theta_c = 4\pi/KM\tau_D^{1/2}$ when l_0 is finite [23].

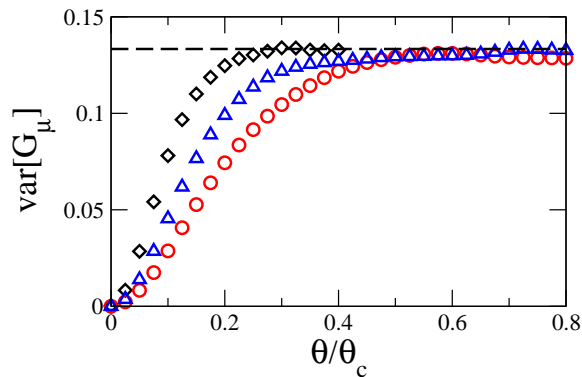


Figure 3: Spin conductance fluctuations for the quantum kicked rotator with SOI defined in Eq. (11) vs. the rescaled TRS breaking parameter θ/θ_c for $N_R = N_L = 1$. For $\theta = 0$, one is in the $\beta = 4$ ensemble and TRS forces the spin conductance to vanish [22]. Breaking TRS results in a finite variance of the spin conductance. Dashed line: RMT prediction $\text{var}[G_\mu] = 4/30$ for $N_R = N_L = 1$ [see Eq. (10b)]. Data correspond to $K = 45$, $K_{\text{so}} = 120 K_{\text{soc}}$, with $M = 128$ (red circles), 256 (blue triangles) and 512 (black diamonds). The curves do not lie on top of one another, because the rescaling of the horizontal axis with θ_c assumes $N_{R,L} \gg 1$ [23].

In our numerics we fix $l_0 = 0.14$. When $K \gg 1$ and $\theta/\theta_c \gg 1$, the charge conductance properties are those of the $\beta = 2$ ensemble, while for $\theta = 0$ and $K_{\text{so}}/K_{\text{soc}} \gg 1$ they are those of the $\beta = 4$ ensemble [23]. In our numerics, we fix $K_{\text{so}}/K_{\text{soc}} = 120$ and vary θ to gradually break TRS, starting from $\theta = 0$. For simplicity, we specify to two-terminal setups and accordingly calculate the dimensionless spin conductance defined by Eq. (3) as $G_\mu = \mathcal{T}_{\text{RL}}^{(\mu)}$ for $\mu = z$. We checked, but do not show, that numerical results remain the same if instead we consider $\mu = x, y$.

Fig. 2 first shows data for quantum corrections to the charge and spin conductance, as TRS is gradually broken. The top panel shows that weak localization corrections to the charge conductance are damped by a Lorentzian $\sim [1 + (\theta/\theta_c)^2]^{-1}$ as predicted by RMT [4] and semiclassics [14]. There is no weak localization correction to the average spin conductance, both with and without TRS, in agreement with Ref. [6]. The bottom panel shows that charge conductance fluctuations are halved upon TRS breaking and their behavior agrees well with theoretical predictions. The situation is entirely different, however, for the spin conductance fluctuations, which are essentially insensitive to the breaking of TRS. This is in agreement with our predictions, Eqs. (7) and (10) for the large number of channels $N > 10$ considered in all data in Fig. 2. The new universal behavior corresponding to broken SRS and TRS emerges at larger θ , where the charge conductance corresponds to the $\beta = 2$ Dyson ensemble, while the spin conductance is essentially the same as that of the $\beta = 4$ ensemble.

Fig. 3 best illustrates the new universal behavior. When the exit lead carries a single transport channel,

TRS	SRS	Charge transport	Spin transport
Yes	Yes	$\beta = 1$	$\beta = 1$; $G_\mu \equiv 0$
Yes	No	$\beta = 4$	$\beta = 4$; Eqs. (9) and (10c)
No	Yes	$\beta = 2$	$G_\mu \equiv 0$
No	No	$\beta = 2$	Eqs. (9) and (10b)

Table I: Universality behavior of charge and spin transport properties in the four possible cases of broken or unbroken SRS and TRS. When both symmetries are broken, the spin transport properties correspond to those of the $\beta = 4$ Dyson ensemble in the limit $N_R, N_L \gg 1$. Deviations from $\beta = 4$ are given in Eq. (10) for the spin conductance variance. They are largest for small number of channels.

TRS requires that the spin conductance vanishes [22], regardless of the presence or absence of SRS. Fig. 3 shows that, when SRS is broken, breaking TRS turns spin currents on, whose variance is given by Eq (10b) once TRS is totally broken. Note that the magnitude of the field necessary to break TRS for $N_{R,L} = 1$ becomes smaller and smaller in the semiclassical limit, $M \rightarrow \infty$ as the dwell time grows in that limit, $\tau_D \sim M$.

Conclusions. By direct calculation we have shown that the spin conductance is an observable that is sensitive to the presence or absence of SRS even when TRS is broken. Breaking of SRS is necessary to magnetoelectrically generate a spin current, thus to acquire a finite spin conductance, but the latter is affected by TRS only when there are very few transport channels. Accordingly, we conclude that the $\beta = 2$ universality class splits into two different subsets for spin transport. In both cases, charge transport properties correspond to the $\beta = 2$ class, however, the spin conductance vanishes identically when SRS is preserved, but exhibits a universal behavior when it is broken, see Eq. (10b). Spin and charge transport universality classes are related to TRS and SRS in Table. I. Examples of systems with broken SRS and TRS include spin-orbit coupled systems under not too strong external magnetic fields, systems with spin textures and even spin valves with non-aligned magnetizations. Breaking TRS without breaking SRS is possible in systems with orbital magnetic field effects stronger than Zeeman effects, such as few-channel n-doped GaAs quantum dots in fields of the order of few tens of milliTeslas [4].

We thank M. Büttiker for several interesting discussions at various stages of this project.

-
- [1] F.J. Dyson, *J. Math. Phys.* **3**, 1199 (1962).
 - [2] Quaternions are numbers that extend the complex numbers. A quaternion Q can be represented as a linear combination of the Pauli and the 2×2 identity matrices, $Q = a_0\mathcal{J} + ia_x\sigma^{(x)} + ia_y\sigma^{(y)} + ia_z\sigma^{(z)}$. A quaternion matrix is a matrix whose matrix elements are quaternions. See e.g. Ref. [3].
 - [3] M.L. Mehta, *Random Matrices*, Academic Press (1991).

- [4] C.W.J. Beenakker, *Rev. Mod. Phys.* **69**, 731 (1997).
- [5] I.L. Aleiner and V.I. Fal'ko, *Phys. Rev. Lett.* **87**, 256801 (2001).
- [6] J.H. Bardarson, İ. Adagideli, and Ph. Jacquod, *Phys. Rev. Lett.* **98**, 196601 (2007).
- [7] Y.V. Nazarov, *New J. Phys.* **9**, 352 (2007).
- [8] J.J. Krich and B.I. Halperin, *Phys. Rev. B* **78**, 035338 (2008).
- [9] İ. Adagideli, J. Bardarson, and Ph. Jacquod, *J. Phys: Condens. Matter* **21**, 155503 (2009).
- [10] J.J. Krich, *Phys. Rev. B* **80**, 245313 (2009).
- [11] J.G.G.S. Ramos, A.L.R. Barbosa, D. Bazeia, M.S. Hussein, and C.H. Lewenkopf, *Phys. Rev. B* **86**, 235112 (2012).
- [12] E.V. Shuryak and J.J.M. Verbaarschot, *Nucl. Phys.* **A560**, 306 (1993).
- [13] A. Altland and M.R. Zirnbauer, *Phys. Rev. B* **55**, 1142 (1997).
- [14] H.U. Baranger, R.A. Jalabert, and A.D. Stone, *Phys. Rev. Lett.* **70**, 3876 (1993); K. Richter and M. Sieber, *Phys. Rev. Lett.* **89**, 206801 (2002); İ. Adagideli, *Phys. Rev. B* **68**, 233308 (2003); S. Heusler, S. Müller, P. Braun, and F. Haake, *Phys. Rev. Lett.* **96**, 066804 (2006); Ph. Jacquod and R.S. Whitney, *Phys. Rev. B* **73**, 195115 (2006).
- [15] P.W. Brouwer and S. Rahav, *Phys. Rev. B* **74**, 075322 (2006).
- [16] O. Zaitsev, D. Frustaglia, and K. Richter, *Phys. Rev. B* **72**, 155325 (2005); J. Bolte and D. Waltner, *Phys. Rev. B* **76**, 075330 (2007).
- [17] İ. Adagideli, Ph. Jacquod, M. Scheid, M. Duckheim, D. Loss, and K. Richter, *Phys. Rev. Lett.* **105**, 246807 (2010).
- [18] See Supplemental Material at <http://link.aps.org/supplemental/10.1103/PhysRevB.88.041305> for more details on the semiclassical calculation of spin conductance and spin conductance fluctuations, as well as on the kicked rotator model of quantum transport.
- [19] F. Haake, *Quantum Signatures of Chaos*, 2nd Ed., Springer (Berlin, 2001).
- [20] H. Mathur and A.D. Stone, *Phys. Rev. Lett.* **68**, 2964 (1992).
- [21] P.W. Brouwer and C.W.J. Beenakker, *J. Math. Phys.* **37**, 4904 (1996).
- [22] A.A. Kiselev and K.W. Kim, *Phys. Rev. B* **71**, 153315 (2005); F. Zhai and H.Q. Xu, *Phys. Rev. Lett.* **94**, 246601 (2005).
- [23] J.H. Bardarson, J. Tworzydło, and C.W.J. Beenakker, *Phys. Rev. B* **72**, 235305 (2005).
- [24] J. Tworzydło, A. Tajic, H. Schomerus, and C. W. J. Beenakker, *Phys. Rev. B* **68**, 115313 (2003); Ph. Jacquod and E.V. Sukhorukov, *Phys. Rev. Lett.* **92**, 116801 (2004).
- [25] F. M. Izrailev, *Phys. Rep.* **196**, 299 (1990).
-

Supplemental Material

Semiclassical approach to spin transport.

The short-wavelength semiclassical approach to transport has been pioneered by Stone and collaborators, and further developed to include quantum corrections by Richter and Sieber [14]. It is based on the scattering approach to transport, where transmission amplitudes are replaced with their semiclassical expression

$$t_{ij} = \int_i dy \int_j dy_0 \sum_{\gamma} A_{\gamma} \exp[iS_{\gamma}]. \quad (\text{S1})$$

The sums run over all trajectories starting at point y_0 located at the cross-section of the injection lead j and ending at point y at the cross-section of the exit lead i . The stability of the trajectory γ is given by A_{γ} , which includes a prefactor $(2\pi i\hbar)^{-1/2}$ as well as a Maslov index [19], and S_{γ} is the classical action accumulated on γ , in units of \hbar . Charge conductances in units of twice the conductance quantum $2e^2/h$ are given by the transmission probability $|t_{ij}|^2$ which contains a double sum over trajectories and four spatial integrals. In the semiclassical, short-wavelength limit, these integrals reduce to two integrals [14], and one has

$$T_{ij} = |t_{ij}|^2 = \int_i dy \int_j dy_0 \sum_{\gamma, \gamma'} A_{\gamma} A_{\gamma'} \exp[i(S_{\gamma} - S_{\gamma'})]. \quad (\text{S2})$$

Noting that the stability is much less energy-dependent than S_{γ} , the integrals in the above expression for $\langle T_{ij} \rangle$ (averaged over a small, but finite energy interval) are evaluated via a stationary phase approximation which results in specific pairings of the trajectories γ and γ' [14]. For the conductance fluctuations, one obtains

$$\text{var}T_{ij} = \left\langle \left(\int_i dy \int_j dy_0 \sum_{\gamma, \gamma'} A_{\gamma} A_{\gamma'} \exp[i(S_{\gamma} - S_{\gamma'})] \right)^2 \right\rangle - \langle T_{ij} \rangle^2. \quad (\text{S3})$$

After a stationary phase approximation, this expression requires the pairing of four trajectories. The terms corresponding to disconnected pairings are cancelled by $-\langle T_{ij} \rangle^2$. One is left with the five contributions shown in Fig.1 of the main text. They were calculated in Ref. [15], which furthermore showed that the sum of contributions c), d) and e) vanish. Thus only contributions a) and b) matter for the charge conductance. Contribution b) vanishes when time-reversal symmetry is broken, thus the variance of the conductance is divided by two.

The presence of spin-orbit interaction forces one to include spin rotation into the semiclassical propagator of Eq. (S1). In the weak spin-orbit coupling limit one usually makes the approximation in which the sole effect of the spin-orbit field is to rotate the spin along the unchanged classical trajectories. Mathur and Stone therefore replaced Eq. (S1) by

$$t_{i\sigma, j\sigma'} = \int_i dy \int_j dy_0 \sum_{\gamma} A_{\gamma} \exp[iS_{\gamma}] (U_{\gamma})_{\sigma, \sigma'}, \quad (\text{S4})$$

with $U_{\gamma} \in SU(2)$ encoding the spin rotation. The average charge conductance, this time in units of the conductance quantum e^2/h , is given by,

$$\sum_{\sigma, \sigma'} |t_{i\sigma, j\sigma'}|^2 = \int_i dy \int_j dy_0 \sum_{\gamma, \gamma'} A_{\gamma} A_{\gamma'} \exp[i(S_{\gamma} - S_{\gamma'})] \text{Tr}[U_{\gamma'}^{\dagger} U_{\gamma}], \quad (\text{S5})$$

and its average is usually calculated by performing the average separately over orbital and spin degrees of freedom. Thus, in order to account for the spin-orbit effects, one multiplies the right-hand side of Eq. (S2) by $\langle \text{Tr}[U_{\gamma'}^{\dagger} U_{\gamma}] \rangle_{SU(2)}$. The leading-order contribution to the charge conductance is given by the diagonal approximation, $\gamma = \gamma'$, with $\langle \text{Tr}[U_{\gamma}^{\dagger} U_{\gamma}] \rangle_{SU(2)} = \text{Tr}[I_{2 \times 2}] = 2$ for spin 1/2 particles. The weak localization correction corresponds to the diagram shown in Fig. S1, which is multiplied by $\langle \text{Tr}[U_{\text{loop}}^2] \rangle_{SU(2)} = -1$ [16]. If there is no spin rotation (in the absence of spin-orbit interaction), one instead obtains 2. This explains the magnitude and sign reversal of magnetoresistance with/without spin-orbit interaction. There are different ways to calculate such averages over $SU(2)$. For instance one may write

$$U_{\text{loop}} = \begin{pmatrix} \alpha & \beta \\ -\beta^* & \alpha^* \end{pmatrix},$$

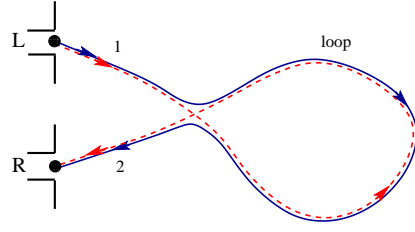


Figure S1: (Color online) Semiclassical diagram determining the weak localization contribution to the conductance and spin conductance, to leading order in the number $N \gg 1$ of transport channels. Blue (dark) and red (light) trajectories travel in opposite direction along the loop, thus the contribution vanishes in the presence of a large magnetic flux piercing the loop, giving rise to magnetoresistance.

with $|\alpha|^2 + |\beta|^2 = 1$, so that real and imaginary parts of α and β correspond to coordinates on a 3-sphere. The average can then be calculated via an integral over the surface of that sphere.

For spin transport, on the other hand, the additional factor to calculate becomes $\langle \text{Tr}[U_{\gamma'}^\dagger \sigma^{(\mu)} U_{\gamma}] \rangle_{\text{SU}(2)}$. This average vanishes for both the diagonal and the weak localization contributions to the conductance [17]. For spin conductance fluctuations, the factors are obtained by labeling different trajectory segments. This is done explicitly in Fig. S2. The spin-dependent prefactor is then straightforward to obtain, for the spin conductance fluctuations it is $\langle \text{Tr}[U_1^\dagger U_5^\dagger U_3^\dagger \sigma^{(\mu)} U_3 U_2 U_1] \times \text{Tr}[U_4^\dagger U_2^\dagger U_6^\dagger \sigma^{(\mu)} U_6 U_5 U_4] \rangle = \langle \text{Tr}[U_5^\dagger U_3^\dagger \sigma^{(\mu)} U_3 U_2] \times \text{Tr}[U_2^\dagger U_6^\dagger \sigma^{(\mu)} U_6 U_5] \rangle$. The calculation of this average as an integral over the surface of the 3-sphere does not present any technical difficulty, and one finds that it vanishes. Similar labelling of the other contributions in Fig.1 of the main text lead to the expression giving there, with only contributions d) and e) giving finite values as they are multiplied by a different spin-prefactor.

The kicked rotator model for transport.

Our numerics are based on the spin kicked rotator model. The kicked rotator was introduced in the context of quantum chaos by Casati, Chirikov, Izrailev and Ford (for a review of the kicked rotator in quantum chaos see Ref. [25]). It is a generic model of dynamical systems. It has been extended to study open condensed matter systems [14, 24], where it has in particular been found that all properties expected of ballistic quantum dots can be reproduced (weak localization, universal conductance fluctuations, shot-noise and so forth). It has recently been extended to account for the presence and the influence of spin-orbit interaction on charge transport in Ref. [23], again reproducing expected reversal of magnetoresistance when the spin-orbit interaction is cranked up, the reduction in conductance fluctuations and so forth. Ref. [6] applied the spin kicked rotator to spin transport, and it was found that the model reproduces random matrix theory predictions in a wide range of parameters.

The Hamiltonian for the kicked rotator is

$$H = \frac{(k + l_0)^2}{2} + K \cos(p + \theta) \sum_n \delta(t - n\tau_0), \quad (\text{S6})$$

which represents a free particle with kinetic energy $(k + l_0)^2/2$ periodically perturbed by kicks of strength K and period τ_0 . The latter time scale just serves as a unit of time from now on and we accordingly set it equal to one. The parameters l_0 and θ are necessary to break time-reversal symmetry [25]. Because of the system's additional symmetries two, and not one (e.g. magnetic field) parameters are necessary to break time-reversal symmetry. The Hamiltonian is quantized on a torus by discretizing momenta, $k \rightarrow k_l = 2\pi l/M$, $l = 1, 2, \dots, M$, and positions $p \rightarrow p_n = 2\pi n/M$. The model is usually represented by its Floquet, unitary time-evolution operator from the middle of a free evolution period to the middle of the next one. In this way the Floquet operator is symmetrized. Momentum and position are

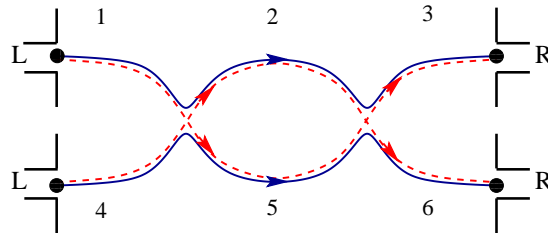


Figure S2: (Color online) Contribution a) of Fig.1 of the main text to the conductance fluctuations. Different trajectory segments are explicitly labelled.